ARTICLE
Journal of Cellular Biochemistry 110:129–140 (2010)

Journal of Cellular Biochemistry

More Insights Into the CCN3/Connexin43 Interaction Complex and Its Role for Signaling

Alexandra Gellhaus,[1*] Christoph Wotzlaw,[2] Teresa Otto,[2] Joachim Fandrey,[2] and Elke Winterhager[1]

[1]*Institute of Molecular Biology, University of Duisburg-Essen, Hufelandstrasse 55, D-45122 Essen, Germany*

[2]*Institute of Physiology, University of Duisburg-Essen, Hufelandstrasse 55, D-45122 Essen, Germany*

ABSTRACT

Connexin43 (Cx43) forms gap junction channels but also serves as a signaling center by binding to proteins via its C-terminus. We have previously demonstrated that transfection of Cx43 leads to significantly reduced proliferation of placental tumor cells through upregulating and binding of the growth regulator CCN3 (NOV) at the C-terminus of Cx43. Here, we combined fluorescence resonance energy transfer (FRET), co-immunoprecipitation and proliferation and expression assays to characterize the interaction complex of Cx43 and CCN3. FRET measurements confirmed the interaction of CCN3 with wild-type Cx43 (amino acids 1-382) and with mutants of Cx43 truncated at the C-terminus resulting in Cx43 proteins of amino acids 1-374, 1-273, 1-264, 1-257 in 293T cells. These results matched the co-immunoprecipitation data. Interestingly, although FRET revealed distinct efficiencies in interaction of Cx43 with CCN3 for all deletion constructs only wild-type Cx43 and one deletion construct (1-374) led to increased CCN3 expression. Only these interactions which were associated with increased CCN3 expression resulted in a reduced cell proliferation. Our study provides evidence that only defined binding properties between Cx43 and CCN3 leading to an upregulation of CCN3 are needed for signaling. Furthermore, the data obtained by FRET analysis allowed us to model the 3D structure of the C-terminus of Cx43 interacting with CCN3. J. Cell. Biochem. 110: 129–140, 2010.

KEY WORDS: CCN3; CX43; GAP JUNCTION; FLUORESCENCE RESONANCE ENERGY TRANSFER (FRET); PROTEIN INTERACTION; CELL PROLIFERATION

Protein–protein interactions are crucial for establishing signaling pathways for almost all cellular processes. To determine where and how a protein interacts with its partner will provide significant insights into the initiation of signaling pathways. Gap junctional connexin proteins do not only enable cells to directly cooperate both electrically and metabolically but are thought to serve as signaling proteins acting via its cytoplasmic C-terminus. Several lines of evidence indicate that gap junctions are important for regulating cell growth and differentiation and for maintaining tissue homeostasis [Loewenstein, 1972]. Recently, a growing number of reports indicate that tumorigenesis is associated with decreased or missing gap junctions [Mesnil et al., 2005; Leithe et al., 2006; Sato et al., 2008]. However, defined molecular mechanisms how the gap junction channel can interfere with the cell-cycle regulation have remained elusive.

Gap junctions are plasma membrane bound intercellular channels composed of 12 connexin proteins forming a water filled pore for the exchange of ions and small molecules such as second messengers including siRNA [Harris, 2007; Mese et al., 2007; Dbouk et al., 2009]. Until now, 20 connexin genes have been identified in the mouse and 21 in the human genome [Soehl and Willecke, 2003, 2004]. The different types of connexin channels can differ in the permeability for one specific molecule [Harris, 2007]. Though the transmembrane part and the extracellular loops are highly conserved among the different connexin isoforms the carboxyl terminus is most variable in length and amino acid sequence. The carboxyl terminus of several connexins contains various phosphorylation sites which play an important role in regulating gap junction channel conductivity and function [Moreno and Lau, 2007; Solan and Lampe, 2009].

Abbreviations used: Cx43, connexin43; FRET, fluorescence resonance energy transfer; CCN3; NOV, nephroblastoma overexpressed.

Alexandra Gellhaus and Christoph Wotzlaw contributed equally to this work.

Additional Supporting Information may be found in the online version of this article.

Grant sponsor: German Research Foundation (DFG); Grant number: Wi 774/21-3; Grant sponsor: European Commission under the 6th Framework Programme; Grant numbers: LSHM-CT-2005-018725, PULMOTENSION.

*Correspondence to: Dr. Alexandra Gellhaus, PhD, Institute of Molecular Biology, University of Duisburg-Essen, Hufelandstrasse 55, D-45122 Essen, Germany. E-mail: alexandra.gellhaus@uk-essen.de

Received 19 October 2009; Accepted 6 January 2010 • DOI 10.1002/jcb.22519 • © 2010 Wiley-Liss, Inc.

Published online 24 March 2010 in Wiley InterScience (www.interscience.wiley.com).

Recently, a channel-independent role for connexins in intracellular signaling was suggested [Giepmans, 2004; Kardami et al., 2007; Dbouk et al., 2009]. Up to now several interaction partners are known to bind to the Cx43 tail, for example, ZO-1, c-Src, tubulin, drebrin, and CIP75 [Giepmans and Moolenaar, 1998; Giepmans et al., 2001a,b; Toyofuku et al., 2001; Butkevich et al., 2004; Li et al., 2008]. The interaction of ZO-1 with Cx43 is probably required for appropriate assembly and stabilization of Cx43 gap junctions [Toyofuku et al., 1998; Hunter et al., 2005]. Analysis of the specific binding domains in the C-termini of the different interaction partners of Cx43 indicated that positions -3 and -2, and the final hydrophobic amino acid at the C-terminus of the PDZ2 domain, are critical for ZO-1 binding [Jin et al., 2004; Chen et al., 2008]. Though the binding sites for ZO-1 and c-Src are separated by about 100 amino acids c-Src can disrupt this Cx43-ZO-1 interaction, leading to downregulation of gap junction intercellular communication which points to a multimolecular complex for action [Sorgen et al., 2004]. Interestingly, these results differ from interactions with Cx40 because the Cx40/ZO-1/PDZ2 complex was unaffected by SH3/c-Src domain and both domains interacted simultaneously with the C-terminus of Cx40 suggesting different mechanisms of regulation between the connexin isoforms [Bouvier et al., 2008].

It was demonstrated that, independently from gap junction channel formation, the Cx43 protein itself is able to affect growth control. Moorby and Patel [2001] showed that the C-terminus of Cx43 (243-382aa) alone is as effective as the full-length protein in suppressing neuroblastoma cell growth.

The mostly unique and tissue-specific functions of the connexin channels have been found by generating connexin-deficient mice as well as by exchanging connexin isoforms [Willecke et al., 2005]. Multiple phenotypes support the hypothesis of additional channel independent functions which are cell and tissue specific. In recent publications [McLeod et al., 2001; Fu et al., 2004; Gellhaus et al., 2004] it has been demonstrated that in communication-deficient tumor cells restoration of the gap junction channels by transfection of Cx43 significantly reduced tumor proliferation and tumor growth associated with an upregulation of CCN3, a growth regulator protein of the CCN family. We and others could show that this upregulation of CCN3 was combined with a translocation of the protein from the nucleus and cytoplasm to the membrane where it interacts with Cx43 [Fu et al., 2004; Gellhaus et al., 2004; Sin et al., 2009]. Co-immunoprecipitation revealed a binding of CCN3 specifically to the C-terminus of Cx43.

The CCN family belongs to a group of structurally related proteins which are not only intracellularly located but are also secreted and bind to the extracellular matrix defining an important role for members of this family in internal and external cell-signaling pathways. CCN functions seem to be predominantly mediated via extracellular cell adhesion receptors such as integrins [Chen and Lau, 2008; Holbourn et al., 2008]. The CCN family consists of six members, *c*ystein-*r*ich 61 (*C*YR61, CCN1), *c*onnective *t*issue *g*rowth *f*actor (*C*TGF, CCN2), *n*ephroblastoma *ov*erexpressed (*N*OV, CCN3) and *W*nt-*i*nduced *s*ecreted *p*roteins (WISP1-3, CCN4-6) which are involved in the regulation of various cellular processes such as proliferation, adhesion, migration, and differentiation [Perbal, 2004; Leask and Abraham, 2006; Katsube et al., 2009]. CCN3 was the first member of the CCN family to show anti-proliferative activity in several tumors such as neuroblastoma, glioma, and chronic myeloid leukemia. In stem cells such as hematopoetic progenitor cells or mesenchymal cells CCN3 acts through the membrane bound Notch receptor to regulate self-renewal and differentiation potential [McCallum and Irvine, 2008; Katsuki et al., 2008].

The binding capacity of CCN3 to the cytosolic C-terminus of Cx43 which results in an increase in CCN3 expression could provide the missing link between connexin expression and the regulation of tumor growth. To analyze the binding properties of CCN3 to the different C-terminus domains required for physiological consequences we have chosen FRET analysis combined with co-immunoprecipitation studies to prove interaction of CCN3 and Cx43 C-terminus in 293T cells.

These approaches were extended by proliferation and expression assays to combine the binding capacities with functional consequences. Only binding to almost the complete C-terminus associated with an increase in CCN3 expression was able to reduce cell proliferation. Our data obtained by FRET analysis together with already known NMR data of the Cx43 C-terminus [Sorgen et al., 2004] let us create a 3D model of the CCN3/Cx43 interaction complex.

MATERIALS AND METHODS

CELL CULTURE AND TRANSIENT TRANSFECTION

Human embryonic kidney epithelial cells (293T) were grown in Dulbecco's modified Eagle medium (DMEM; Invitrogen, USA) supplemented with 10% fetal calf serum and penicillin/streptomycin (10 ml/L). Cells were cultured in 24-well plates on cover slips for FRET studies and without cover slips for cell proliferation analysis. For co-immunoprecipitation analysis as well as immunoblots cells were cultured on 6-well plates.

For transient transfection the appropriate amount of plasmid DNA was mixed with Fugene6 (Roche, Mannheim, Germany) and suspended in appropriate volume of DMEM for each culture dish. Cells were transfected with different DNA constructs for 48 h (FRET, co-immunoprecipitation, expression analyses) and cultured for up to 6 days for proliferation studies. Medium was renewed and all experiments started after 24 h.

PLASMID CONSTRUCTION

The coding sequences of Connexin43 full length (1-382), various C-terminal truncated Cx43 constructs (1-257, 1-264, 1-273, and 1-374) as well as full-length HIF-1α and full-length CCN3 were amplified by polymerase chain reaction (PCR) from pFlag-Cx43 (1-382), pcDNA3-HIF-1α, and pHis-NOV/CCN3 [Gellhaus et al., 2004]. PCR products were ligated into pECFP-N1 and pEYFP-N1 (Clontech, Heidelberg, Germany), respectively, generating the following expression vectors: ECFP-Cx43-WT (1-382), Cx43-257, -264, -273, and -374 (1-257; 1-264; 1-273; 1-374), EYFP-CCN3, and ECFP-HIF-1α with the CFP and YFP tags fused to the C-termini of full length and Cx43 with different truncations of the C-terminus, HIF-1α and CCN3 protein, respectively. All constructs were confirmed by sequencing.

FLUORESCENCE RESONANCE ENERGY TRANSFER (FRET) PROTEIN–PROTEIN INTERACTION ANALYSIS

The interaction analysis between Cx43 or its deletion variants and CCN3 was performed with the sensitized FRET technique. For experiments the confocal Nikon PCM2000 system equipped with two photomultipliers, a 442 nm DPSS laser for ECFP excitation, a 532 nm DPSS laser for EYFP excitation (Crysta Laser, Reno, USA) and the inverse microscope Nikon Eclipse TE300 were used [Wotzlaw et al., 2007]. Image acquisition was performed with a 60×/1.20 water objective (Nikon, Düsseldorf, Germany).

The ECFP signal of Cx43 chimeras after excitation with the 442 nm laser was collected via a 480/30 filter (intensity of the donor, ID), the signal of EYFP-CCN3 after excitation with the 532 nm laser was collected using a 565/40 filter (intensity of the acceptor, IA). All filters were from AHF Analysentechnik AG (Tübingen, Germany). The intensity of the FRET signal (IF) was collected by a photomultiplier with a 565/40 filter after excitation with the 442 nm DPSS laser. FRET efficiency was calculated according to the following equation:

$$\text{FRET efficiency } E = 1 - \left[\frac{\text{ID}}{(\text{ID} + \text{IF} - \text{ID} \times \text{BTD} - \text{IA} \times \text{BTA})}\right] \quad (1)$$

BTD and BTA represent the amount of spectral bleedthrough as described by Feige et al. [2005].

For automated data analysis the software package $_{\text{TRUE}}$FRET V10 was programmed. Algorithms were included to balance for inhomogeneous scan area illumination and to allow automated detection of background. Results are presented as a graph showing the mean FRET efficiency of a cell calculated from Equation (1) as a function of the ratio of the intensities in the EYFP (acceptor) channel to that in the ECFP (donor) channel. The correlation between the emission signal values and real amount of the fluorophores was determined with a tandem construct with one EYFP and one ECFP molecule spaced by an intermediate short protein (PIN1; ECFP-2 amino acids (aa)-PIN1 (161 aa)-2 aa-EYFP).

GFP and its derivatives (e.g., ECFP and EYFP) tend to dimerize via hydrophobic interaction, especially at higher concentrations [Zacharias, 2002]. This defines the biochemical limit of detection of signal due to molecular interaction. To determine the detection limit of our scanning system 293T cells were co-transfected with the empty control vectors pECFP-N1 and pEYFP-N1 (Invitrogen, Karlsruhe, Germany). Twenty-five cells were scanned to determine FRET efficiency values as a function of the acceptor EYFP/donor ECFP ratio (A/D). The graph is described by a three parameter sigmoidal function in a multi-donor-multi-acceptor system [Feige et al., 2005]. Regression analysis by Sigmaplot 2001 software (Systat Software GmbH, Germany) resulted in a FRET efficiency of 8.6% at the plateau value. Graphs were calculated for the sigmoidal relationship between the FRET efficiency and the ratio A/D of EYFP-CCN3/ECFP-Cx43 signals according to:

$$\text{FRET efficiency } E = \frac{a}{\left[1 + e^{-((A/D - x_0)/b)}\right]} \quad (2)$$

where A/D, a and b represent the three parameters of the function. Values for x_0 and b were taken from cells co-transfected with ECFP-N1 and EYFP-N1. For each construct a combination of 6–15 cells was analyzed.

In a system of one donor and one acceptor molecule the distance between both fluorophores can be calculated using the formula:

$$R = R_0((1/E) - 1)^{1/6} \quad (3)$$

where R is the distance between the donor and acceptor and R_0 is the distance at which 50% of the energy is transferred characterizing the properties of the used dyes. R_0 was set to 4.92 nm (Patterson et al., 2000). R_0 covers the relative orientation between the two dyes and is called κ^2. It is known that the dipole moments of donor and acceptor molecules are free to rotate in all directions which result in a geometric averaging of the angles: $\kappa^2 = 2/3$.

For the modeling we assumed that in a biological system with several fusion proteins only the nearest acceptor fluorophore attached to the CCN3 interacting with its chimeric Cx43 counterpart is absorbing energy from the Cx43 donor fluorophore during the FRET process. This allows the calculation of distances between fluorophores using formula (3). The plateau of the graph reflects the state of no competition of donor molecules for an acceptor molecule during the FRET process. These maximum FRET efficiency values were taken for calculation of mean distances between the C-terminal localized fluorophores at the Cx43 and CCN3 molecules.

For the graphical visualization of the relative positions of Cx43 and CCN3 C-termini NMR data of the Cx43 C-terminus [Sorgen et al., 2004] were implemented into Cinema 4D (Maxon Computer GmbH, Germany) used for 3D modeling of interaction complexes.

IMMUNOBLOT ANALYSIS

Whole protein extracts were prepared with NETN lysis buffer (20 mM Tris/HCl, pH 8, 100 mM NaCl, 0.5% NP-40, 1 mM EDTA) supplemented with EDTA free complete protease inhibitors (Roche, Penzberg, Germany). Protein content was quantitated using the Bio-Rad protein assay reagent. After addition of one-fourth of volume of 4× sample buffer (50 mM Tris, pH 6.8, 2% sodium dodecyl sulfate, 5% β-mercaptoethanol, 0.0125% bromphenol blue, and 1% glycerine), samples were subjected to 10% polyacrylamide gel electrophoresis, and transferred to a nitrocellulose membrane (Whatman, Schleicher & Schuell, Dassel, Germany). Blots were stained with Ponceau S solution (Bio-Rad, Munich, Germany) to ensure equal protein loading and transfer. Membranes were blocked with 5% non-fat dried milk in Tris-buffered saline (TBS) with 0.15% Tween-20 and incubated with the primary antibody. The following primary antibodies were used: monoclonal mouse anti-Cx43NT1 (clone P1E11; FHCRC, Washington, USA), polyclonal CCN3 anti-serum raised in rabbits against the full-length CCN3 protein (affinity-purified; generated by N. Schuetze, Würzburg, Germany and A. Gellhaus), monoclonal CCN3 anti-serum raised in goats (R&D Systems, Wiesbaden, Germany), monoclonal anti-HIF-1α (BD Biosciences, Heidelberg, Germany), and polyclonal rabbit anti-actin (Sigma–Aldrich, Steinheim, Germany) for normalization of protein expression. Secondary antibodies were anti-rabbit and anti-mouse IgG antibody conjugated to horseradish peroxidase

(Santa Cruz Biotechnologies, Heidelberg, Germany). Immunoreactive proteins were visualized using the luminol coumarin acid H_2O_2 system (per membrane: 12.5 μl 90 mM coumarin acid, 25 μl 250 nM luminol, 1.5 μl 30% H_2O_2 in 5 ml 100 mM Tris/Cl, pH 8.5) and ECL Advanced System (GE Healthcare, Munich, Germany) followed by exposure to X-ray film (Agfa, Cologne, Germany).

CO-IMMUNOPRECIPITATION (CO-IP)

293T cells were transiently co-transfected with EYFP-CCN3 and the different ECFP-Cx43 labeled constructs (wild-type or variants) with Fugene6 (Roche, Mannheim, Germany) and harvested 48 h after transfection by lysis of the cells in 100 μl NETN lysis buffer (see above) per well at 4°C. Samples were incubated on ice for 20 min, ultrasonicated for 3 × 1 min, centrifuged at 15,000*g* for 10 min, and the supernatant was transferred to a fresh tube. To preclear the lysates to lower the amount of non-specific contaminants in the cell lysates and to remove proteins with high affinity for Protein G or Protein A, 30 μl of protein A/G agarose (Santa Cruz Biotechnology, Heidelberg, Germany) was added and the samples were incubated overnight at 4°C on a Rotator (Labnet, NJ, USA). Tubes were spun at 4°C and 15,000*g* for 5 min, the precleared lysate was transferred to a fresh tube and protein content was quantitated using the Bio-Rad protein assay reagent. One to 5 μg polyclonal anti-CCN3 was added to the precleared lysates and the samples were incubated overnight at 4°C on a Rotator. As a control, 10 μl of precleared homogenate was collected for the immunoblot analysis, corresponding to a 1:100 dilution of the initial amount subjected to the immunoprecipitation reaction. As a further control we used PBS buffer instead of anti-CCN3 for the immunoprecipitation reaction as well as cells transfected with ECFP-labeled HIF-1α instead of the different Cx43 constructs which has no affinity to CCN3.

The next day, 50 μl of protein A/G agarose was added and the samples were incubated at 4°C for 2 h on a rotator. The CCN3 antibody–protein A/G agarose complex was spun down at 15,000*g* for 1 min and washed with PBS for five times containing 2× Complete® proteinase inhibitor minimizing electrophoresis artefacts due to ionic composition during SDS–PAGE. Thirty microliters of 4× sample buffer (see above) was added to the precipitate, samples were incubated at 95°C for 10 min and spun at 15,000*g* for 2 min to pellet the protein A/G immunocomplex. Fifteen microliters of supernatant per sample was subjected to a 10% polyacrylamide gel electrophoresis and co-immunoprecipitates were investigated using monoclonal mouse anti-Cx43NT1 (clone P1E11, FHCRC) and polyclonal rabbit anti-CCN3 as primary and horseradish peroxidase-conjugated goat anti-mouse or goat anti-rabbit IgG as secondary antibodies (Santa Cruz Biotechnology). Four independent experiments were performed.

IN VITRO PROLIFERATION ASSAY

For analysis of cell proliferation 293T cells were plated at a density of 5×10^4 cells/well in 24-well plates in triplicate, were transfected with different ECFP-labeled Cx43 constructs and were counted at day 1, 3, and 6 after transfection using a CASY cell counter (Casy1; Schaerfe System, Reutlingen, Germany). As controls for stable expression of the transfected constructs protein expression was primarily checked by immunoblotting and localization of the ECFP-labeled Cx43 proteins. To test the expression of the different transfected Cx43 constructs cells were plated on cover slips, fixed at the indicated time points of 1, 3, and 6 days after transfection, mounted in Mowiol (Roth, Karlsruhe, Germany) and studied using a confocal laser-scanning microscope (LSM 510; Zeiss, Germany).

STATISTICAL ANALYSIS

If not otherwise mentioned data for statistical significance were analyzed by the Mann–Whitney test for non-parametric independent two-group comparisons with the program SPSS 16 for Windows (SPSS, Inc., Chicago, IL). Differences with a *P*-value ≤ 0.05 were regarded as statistically significant.

RESULTS

CHARACTERIZATION OF THE C-TERMINUS TRUNCATED CX43 CONSTRUCTS

Previously we demonstrated that restoration of communication properties via Cx43 in a placental tumor cell line led to a significant reduction of tumor proliferation and growth [Gellhaus et al., 2004]. This was associated with binding of CCN3 (NOV) to the C-terminus of Cx43 in the region between 257 and 382 amino acids combined with an upregulation of CCN3 expression.

In order to narrow down the binding site, Cx43 constructs with truncations of the C-terminus of Cx43 were generated considering already known binding sites for other previously identified interaction proteins of Cx43. In frame Cx43 deletion variants consisting of amino acids 1-257, 1-264, 1-273, and 1-374 (named Cx43-257, Cx43-264, Cx43-273, and Cx43-374) were generated. The Cx43-257 and Cx43-264 deletion variants comprised most parts of the tubulin binding domain (228-263) but contain a deletion of the SH2 (262-267), SH3 (274-284) and the PDZ2 binding domain (378-382) which is the binding site for ZO-1; the Cx43-273 variant covers the tubulin and SH2 binding domain but lacks the SH3 and PDZ domain and the Cx43-374 variant only contains a deletion of the PDZ2 domain. In addition, we used the full-length Cx43 construct (Cx43-WT).

DIFFERENT BINDING CAPACITIES OF ECFP-CX43 DELETION CONSTRUCTS AND EYFP-CCN3 IN 293T CELLS USING FRET ANALYSIS

We used the sensitized FRET technique to analyze the interaction of EYFP-CCN3 and the different ECFP-Cx43 deletion constructs in human embryonic kidney 293T cells.

In Figure 1 the localization of the transfected EYFP-CCN3 proteins and ECFP-Cx43 constructs in 293T cells is exemplarily summarized. The schematic drawing of the different fusion deletion constructs is represented in the first column whereas the FRET efficiency values are encoded in false colors in the right column. In general and irrespective of the transfected Cx43 deletion construct interaction of both proteins was mostly found at membrane borders. To some extent both proteins were also localized in the cytosol surrounding the nucleus, indicating a potential localization in the ER/Golgi system. However, interaction of Cx43 and CCN3 constructs in the cytoplasm were only sparsely observed.

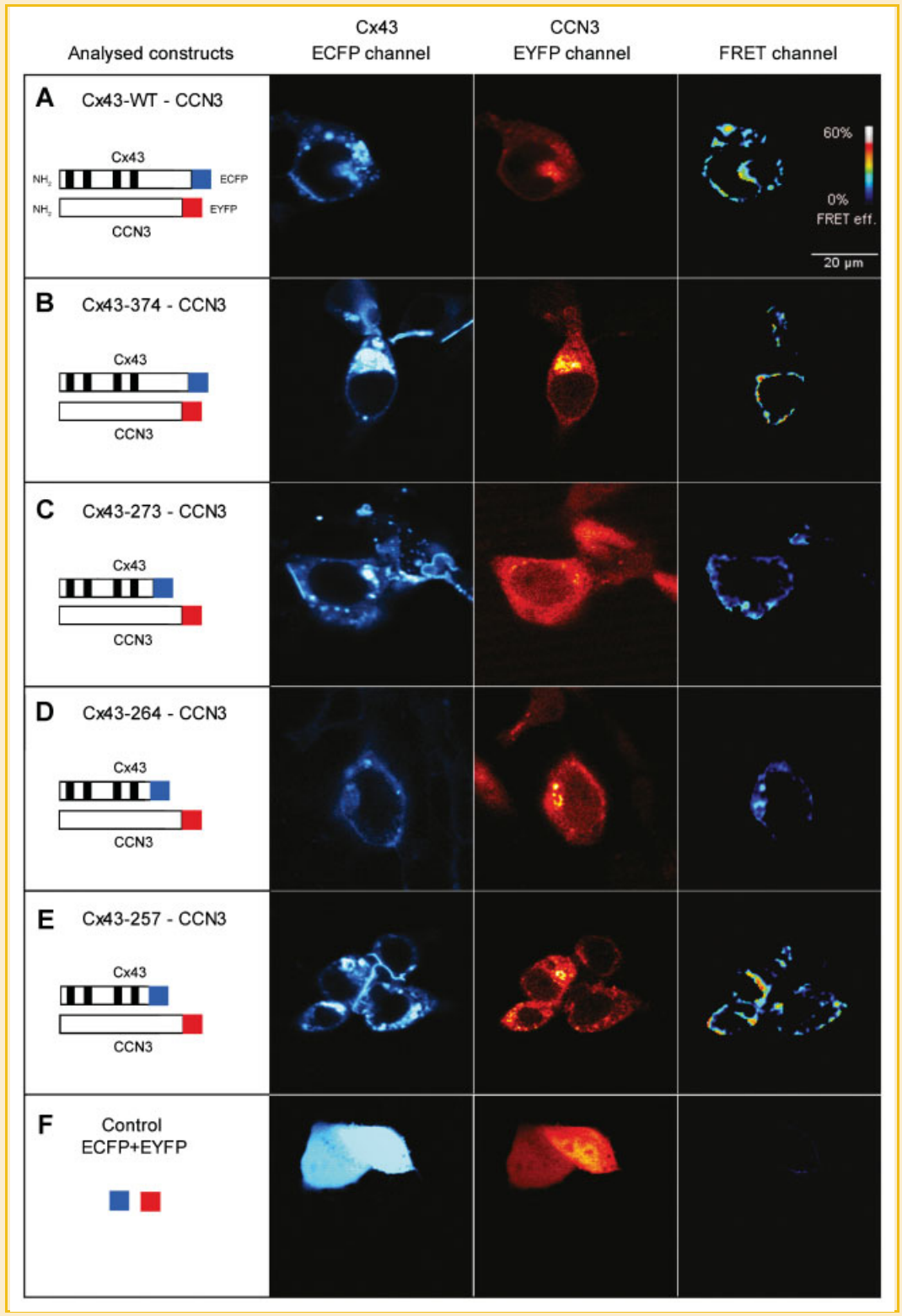

Fig. 1. Localization of ECFP-Cx43 and EYFP-CCN3 fusion proteins in 293T cells and FRET interaction. Localization of ECFP-Cx43 and EYFP-CCN3 fusion proteins in 293T cells is exemplarily shown in the two central columns. The design of the proteins is schematically explained in the left column. For protein–protein interaction analysis the *Fluorescence Resonance Energy Transfer* (FRET) technique and confocal microscopy were used. The right column revealed areas where the laser microscopy system detected signals indicate a potential interaction between Cx43 and CCN3 proteins. The FRET efficiency values are coded in false colors. The mapping is explained in the legend in the upper right image. A–E: Represent specific localization of Cx43 (or deletion mutants) and CCN3 fusion proteins in the cell membrane and cytoplasmic regions (A: Cx43-WT; B: Cx43-374; C: Cx43-273; D: Cx43-264; E: Cx43-257). Cx43-WT (A), Cx43-374 (B), Cx43-257 (E) as well as Cx43-273 (C) showed strong (A,B,E) and moderate (C) FRET efficiency mainly at the cell membrane. The FRET efficiency values were high compared to low values of Cx43-264 (D). F: Low FRET efficiency in 293T cells co-transfected with the empty control vectors pECFP-N1 and pEYFP-N1 due to hydrophobic interaction between the fluorophores.

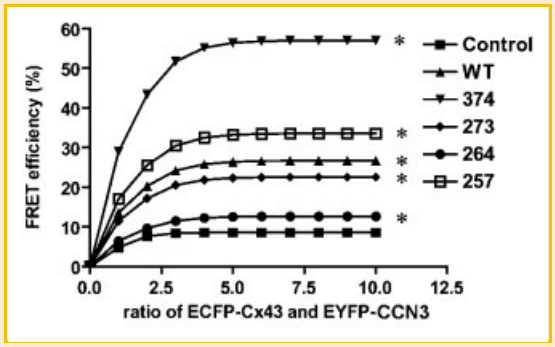

Fig. 2. Different FRET efficiency values in interaction of Cx43 with CCN3 for all Cx43 deletion constructs. Calculated graphs show the typical sigmoidal shape of the curve when mean FRET efficiency values are plotted over the ratio of EYFP-CCN3 to ECFP-Cx43 fusion proteins. The control graph represents experimental data of co-transfected pECFP and pEYFP plasmids delineating random FRET. Graphs above this limit indicate true protein–protein interaction. The highest FRET efficiency graph plateau significantly differs from random FRET (Control) and is represented by Cx43-374 ($N = 9$) followed by Cx43-257 ($N = 15$), Cx43-WT ($N = 6$), and Cx43-273 ($N = 6$). The lowest but significantly different graph from control plateau was that of Cx43-264 ($N = 6$). $^{*}P < 0.05$, significant difference between mean FRET efficiency values of Cx43 and CCN3 co-transfected cells and control cells.

For FRET analysis only single cells which are co-transfected with EYFP-CCN3 and ECFP-Cx43 were chosen. Results from a detailed interaction analysis of selected areas at the cell membrane with 6–15 cells for each construct combination are summarized in Figure 2. Because ECFP and EYFP tend to dimerize via hydrophobic interaction, especially at higher concentrations [Zacharias, 2002], we determine the detection limit of our scanning system, called random FRET, with 293T cells co-transfected with the empty control vectors pECFP-N1 and pEYFP-N1 (Fig. 1F). The graph in Figure 2 shows the typical sigmoidal curves of the mean FRET efficiency values over the ratio of EYFP-CCN3 to ECFP-Cx43 fusion protein fluorescence taking into consideration the different amount of the two transfected fluorophores. Graphs with FRET efficiency higher than the control indicate specific protein–protein interaction. After scanning of all Cx43-CCN3 constructs all pairs showed different plateau levels of FRET efficiency indicating interaction with different proximity of the CCN3 and Cx43 protein.

In Figure 1A the interaction of Cx43-WT and CCN3 was mostly localized at the cell membrane. A subsequent detailed image analysis revealed a heterogeneous distribution of FRET efficiency values at these localizations with some spots showing an efficiency of more than 30% (Fig. 2). The heterogeneity in this interaction intensity within one cell may be due to different acceptor (EYFP-CCN3)/donor (ECFP-Cx43) ratio values or due to temporarily different distances between the fluorophores imaged with the laser microscopy system. The deletion construct Cx43-374 and CCN3 (Figs. 1B and 2) revealed higher FRET efficiency compared to Cx43-WT (see Figs. 1A and 2). Co-localization and resulting FRET efficiency of Cx43-273 (Figs. 1C and 2) and Cx43-264 (Figs. 1D and 2) with CCN3 was lower compared to Cx43-WT and Cx43-374. For the shortest Cx43 deletion construct, Cx43-257, the same co-localization pattern and a moderately higher FRET efficiency (Figs. 1E and 2) as for Cx43-WT (see Figs. 1A and 2) was observed.

In summary, the FRET efficiency for Cx43-264 and CCN3 interaction was lowest, but still significant. Highest FRET intensity was found for interaction of CCN3 with Cx43-374, the construct lacking the PDZ2 domain. FRET efficiencies for CCN3 and Cx43-257, Cx43-WT and Cx43-273 were moderate but significantly higher than for the control.

The data of the different intensities in FRET signals as a function of the acceptor (EYFP-CCN3)/donor (ECFP-Cx43) ratios presented in Figure 2 allow for interpretation of the relative distances of Cx43 and CCN3 C-termini as shown in Table I. FRET efficiency values are primarily a function of the mean distances between the fluorophores, their orientation and spectral characteristics when attached to the C-termini of both molecules. As described (in the Material and Methods Section) the relationship between FRET efficiency and distance between the fluorophores is reciprocal which means the higher the FRET efficiency the lower is the distance between the fluorophores. After scanning of all Cx43-CCN3 constructs all pairs showed different plateau levels above the control (see Fig. 2) indicating different distances between the two molecules (assuming that other factors which may influence the energy transfer mentioned above are in the same range in all experiments). Thus, the results of FRET analysis indicated a small distance between the C-termini of CCN3 and Cx43 fusion proteins. With these data we created a three-dimensional model of the Cx43/CCN3 interaction complex.

3D MODEL OF THE CCN3/CX43 INTERACTION COMPLEX

In Table I the calculated distances between the fluorophores attached to the C-termini of Cx43 mutants and CCN3 are shown. The shortest distance is between the C-terminus of Cx43-374 and the C-terminus of CCN3 (4.7 nm) followed by Cx43-257 (5.5 nm), Cx43-WT (5.8 nm) and Cx43-273 (6.0 nm) whereas the Cx43-264 construct revealed the longest distance (6.8 nm) during interaction with CCN3. These different values were taken into account for the calculation of the interaction complex.

Figure 3A shows a model of the elongated form of the Cx43 C-terminus taken from the NMR data published by Sorgen et al. [2004]. In this Figure 3A the NMR data of the C-terminus of Cx43 are visualized using a CPK model, a kind of calotte model. To give an overview of the relative positions of the last amino acids at the

TABLE I. Calculated Distances Between the Fluorophores Attached to the C-Termini of Cx43 Mutants and CCN3

Interacting molecules	Cx43-WT CCN3	Cx43-374 CCN3	Cx43-273 CCN3	Cx43-264 CCN3	Cx43-257 CCN3
Distance between their C-terminal fluorophores	5.8 nm	4.7 nm	6.0 nm	6.8 nm	5.5 nm

The shortest distance is between the C-terminus of Cx43-374 and the C-terminus of CCN3 (4.7 nm) whereas the Cx43-264 construct revealed the longest distance (6.8 nm) during interaction with CCN3. For more details see the Material and Methods Sections.

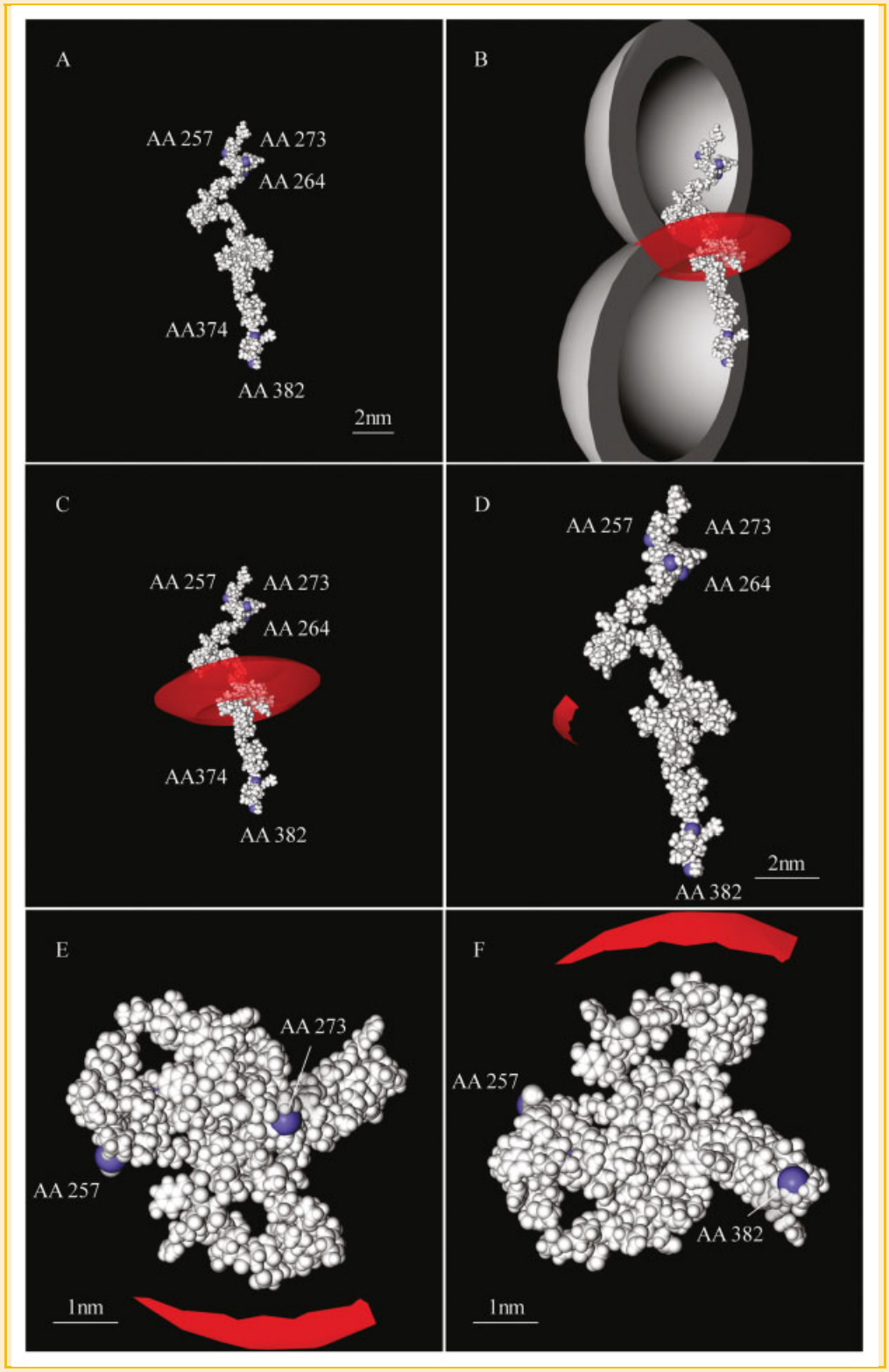

Fig. 3. 3D model of the CCN3/Cx43 interaction complex. Calculation of the putative position of CCN3 C-terminus relative to the C-terminus of cell membrane associated Cx43. The position is deduced from FRET efficiency data (Fig. 2) and NMR data by Sorgen et al. [2004]. In general, the FRET efficiency values are a function of the mean distances between the fluorophores attached to the C-termini of both molecules allowing an estimation of relative positions between the C-termini of proteins. A: CPK model of the C-terminal Cx43. The carboxy terminal carbon of the last amino acids of the Cx43 deletion mutants used in the experiments is labeled in blue, other atoms are labeled in white. B,C: Principle of graphical modeling of the position of the CCN3 C-terminus relative to the C-terminus of Cx43 (for more details see the Results Section). D: The area with the highest probability for the position of the CCN3 C-terminus relative to Cx43 calculated from FRET and NMR data used for the graphical modeling is labeled in red. E,F: Top and bottom views of the three-dimensional arrangement of the Cx43 and CCN3 C-termini (latter is shown in red) in the interaction complex.

C-termini of the different Cx43 deletion mutants the carboxy terminal carbon of each construct is labeled in blue. The plateau values of the FRET efficiency data of each fusion protein pair in graph Figure 2 were used for the calculation of an estimation of distances between the fluorophores inside the fusion proteins [Berney and Danuser, 2003]. Thus, we obtain information of the putative localization of the C-terminus of CCN3 binding to the C-terminus of Cx43 by combining the distance information of the C-termini of all Cx43 variants relative to the CCN3 C-terminus into one 3D model. Figure 3B shows the next step to deduct a three-dimensional graphical model in this case with data from the pairs Cx43-WT/CCN3 and Cx43-257/CCN3 as examples. As mentioned before the plateau values of the FRET efficiency graphs in Figure 2 are taken to calculate distances between the corresponding fluorophores (see the Material and Methods Section). In the graphical model these distance values are interpreted as radii of spheres around the appropriate distal amino acids (Fig. 3B). With respect to the uncertainty implicated in every calculation we used an arbitrary uncertainty factor of 15% expressed by the given thickness of the two axially cropped sphere shapes. The resulting region of overlapping sphere shapes represents the possible localization of the EYFP fluorophore inside the CCN3 fusion protein which is highlighted in red in Figure 3B,C. To locate this area more precisely all FRET data of Figure 2 were then included into the calculation process. The resulting calculated area of the putative position of the CCN3 C-terminus relative to the C-terminal domain of Cx43 appear in red in Figure 3D. The top and bottom views are shown in Figure 3E,F to visualize the interaction complex (for 3D animation of the CCN3/Cx43 interaction complex please refer to the supplementary data). To summarize, our FRET data in combination with the information gained by NMR [Sorgen et al., 2004] let us create a model of the three-dimensional CCN3/Cx43 interaction complex.

MAPPING OF THE CCN3-BINDING REGION IN THE C-TERMINUS OF CX43 BY CO-IMMUNOPRECIPITATION

We transiently transfected embryonic kidney epithelial 293T cells with the ECFP-labeled Cx43-WT and deletion constructs together with full-length EYFP-CCN3—the same constructs as using for FRET. Co-immunoprecipitation was performed on cell lysates with a CCN3 antibody as bait. All Cx43 deletion constructs were precipitated with the CCN3-specific antibody and immunoblotted for Cx43 with an N-terminal specific antibody. Co-IP experiments revealed that all C-terminal deleted Cx43 constructs as well as wild-type Cx43 were able to bind CCN3 in this assay (Fig. 4). We confirmed the specificity of the results by analyzing the precleared lysates of all constructs for expression of EYFP-CCN3 and ECFP-Cx43 (data not shown). Replacing the CCN3 antibody by PBS (C1 in Fig. 4) in the Co-IP approach revealed no binding of CCN3 and Cx43-WT. As a further important control for Co-IP we used ECFP-labeled HIF-1α protein to test the specificity for Cx43 C-terminus binding to CCN3. HIF-1α protein—as an inappropriate binding partner—revealed no binding properties to CCN3 (Fig. 4).

The results of the co-immunoprecipitation data combined with the different controls provide evidence for specific binding of CCN3 to the C-terminus of Cx43 in the region between 257 and 382. However, a preferential binding domain within the Cx43 C-terminus was not identified which confirmed the results obtained by FRET analysis.

UPREGULATION OF ENDOGENOUS CCN3 EXPRESSION UPON ECFP-CX43-WT AND ECFP-CX43-374 TRANSFECTION

As previously shown, induction of Cx43-WT resulted in an upregulation of endogenous CCN3 transcripts [Gellhaus et al., 2004]. Here we ask if and to which extent endogenous CCN3 expression is increased dependent on the different Cx43 deletion constructs. For this investigation we transfected 293T cells only with the different ECFP-labeled Cx43 constructs and analyzed endogenous CCN3 protein expression. Since we observed different transfection efficiencies resulting in different Cx43 expression levels dependent on the Cx43 mutant construct used we normalized the endogenous CCN3 expression level to the amount of transfected Cx43. Our results showed different levels of endogenous CCN3 protein dependent on the different Cx43 deletion constructs (Fig. 5A,B). Compared to the Cx43-257, -264, and -273 constructs we found a twofold significantly higher level of endogenous CCN3

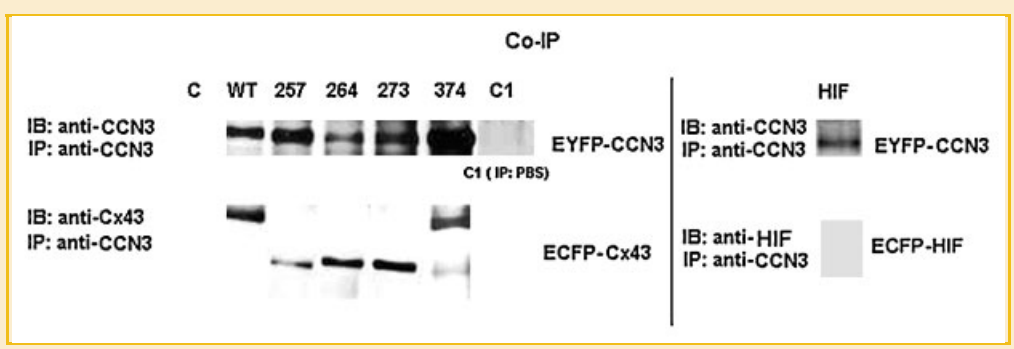

Fig. 4. ECFP-Cx43 variants and EYFP-CCN3 interact in transiently transfected 293T cells using Co-IP. Whole cell lysates were immunoprecipitated (IP) with anti-CCN3 antibody and blotted with anti-Cx43NT1 as well as anti-HIF-1α antibodies (IB). Note that all ECFP-Cx43 truncated constructs (Cx43-257: 55 kDa, -264: 56 kDa, -273: 57 kDa, -374: 68 kDa) as well as the wild-type construct (Cx43-WT: 70 kDa) were specifically immunoprecipitated with EYFP-CCN3 (75 kDa) except for HIF-1α (147 kDa) and the C1 control of Cx43-WT and CCN3 transfected 293T cells (IP: PBS). C: non-transfected cells. One representative immunoblot of four performed independent experiments is shown.

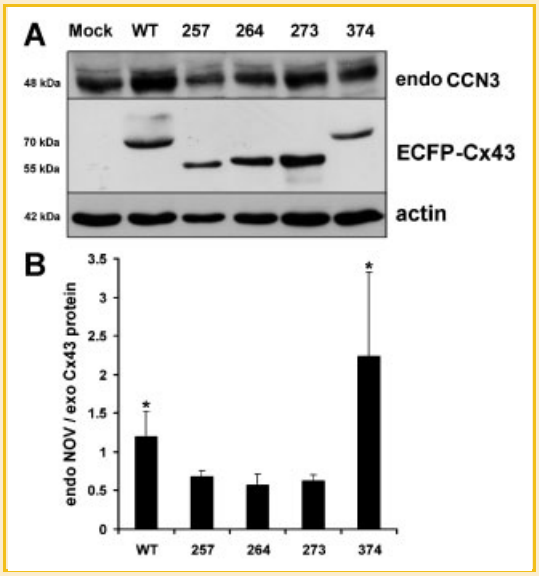

Fig. 5. Upregulation of endogenous CCN3 upon ECFP-Cx43-WT and ECFP-Cx43-374 transfection after normalization to the amount of transfected Cx43. A: Immunoblotting with anti-CCN3 and anti-Cx43NT1 in transfected cells analyzing endogenous CCN3 expression and exogenous ECFP-Cx43 expression. Equal loading of proteins was confirmed by immunoblotting with anti-actin. B: Densitometric analysis of endogenous CCN3 expression normalized to the amount of transfected ECFP-Cx43 (exo Cx43). In detail, endogenous CCN3/actin expression of the cells transfected with the different Cx43 constructs was normalized to the CCN3/actin expression of the mock transfected cells for each of the four experiments. Next, these expression values were further normalized to the Cx43 expression levels of each of the Cx43 constructs. Strong expression of endogenous CCN3 was found in Cx43-WT and Cx43-374 transfected cells where the C-terminus is not deleted (Cx43-WT) or only minimally deleted (Cx43-374) compared to the other C-terminal deleted Cx43 constructs (Cx43-257, -264, -273). One representative immunoblot of four performed independent experiments is shown. $^{*}P < 0.05$, significant difference compared to Cx43-257, -264, and -273 transfected cells.

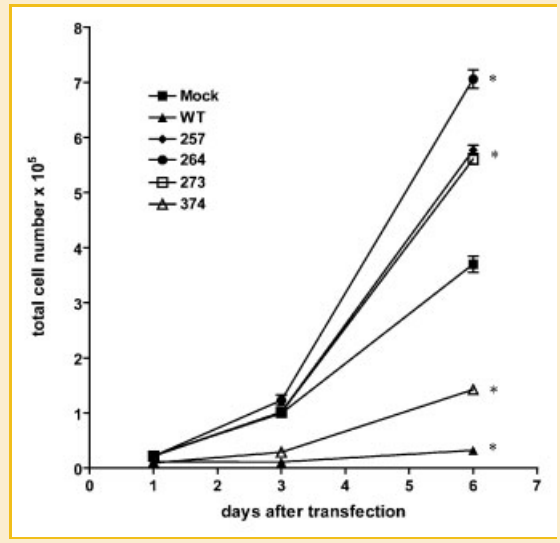

Fig. 6. Reduced proliferation of 293T cells upon ECFP-Cx43-WT and ECFP-Cx43-374 transfection. Cells transfected with Cx43-WT and -374 revealed a significantly reduced cell growth compared to the mock-transfected cells 6 days after transfection, whereas the other Cx43 deletion constructs Cx43-257, -264, and -273 showed an enhanced proliferation rate. $^{*}P < 0.05$, significant difference compared to mock-transfected cells.

expression in Cx43-WT and in Cx43-374 transfected cells (3.9-fold) lacking the PDZ2 domain (Fig. 5B), however, with high variations among the different experiments.

To summarize, the FRET data of the interaction analysis of CCN3 with Cx43-WT and deletion constructs revealed a strong correlation with the positive Co-IP results. However, only transfection with Cx43-WT and Cx43-374 is accompanied by an upregulation of endogenous CCN3.

REDUCED PROLIFERATION OF 293T CELLS UPON ECFP-CX43-WT AND ECFP-CX43-374 TRANSFECTION

Transfection of 293T cells with the various ECFP-labeled Cx43 constructs revealed differences in proliferation properties (Fig. 6). Stable expression of the different constructs was confirmed by immunoblotting of Cx43 protein and by fluorescent microscopy of the Cx43 fusion constructs (data not shown). In addition to previous results in Jeg3 and C6 glioma cells [Gupta et al., 2001; Gellhaus et al., 2004] we now show that in addition transfection of the human embryonic kidney 293T cells with full-length Cx43 protein (Cx43-WT) leads to reduced proliferation (Fig. 6). Significant reduction in proliferation was only found in cells transfected with full-length Cx43-WT and Cx43-374 compared to the mock-transfected cells (Fig. 6) but not with the mutants containing the shorter Cx43 C-terminus domains (Cx43-257, -264, -273) which showed an enhanced proliferative capacity.

To summarize, exclusively expression of Cx43-WT and Cx43-374 constructs which leads to an upregulation of endogenous CCN3 was correlated with a reduced proliferation. In contrast, the shorter deletion constructs Cx43-257, -264, and -273 failed to upregulate CCN3 and did not reduce proliferation.

DISCUSSION

In this study we were able to show for the first time that CCN3/NOV and Cx43 interact in living cells using FRET technology. Our data obtained by FRET analysis allowed us to model the 3D structure of the C-terminus of Cx43 interacting with CCN3/NOV.

Previous studies have already shown that connexin proteins tagged with a fluorescent label at the C-terminus can provide valuable tools for investigating connexins in living cells [Falk and Lauf, 2001; Laird et al., 2001]. In these studies C-terminal tagging of Cx43 allowed normal trafficking and assembly in the membrane to form functional channels. For this reason we used C-terminal tagged constructs of Cx43 for our FRET studies to determine binding with its interaction partner CCN3. FRET technology was already employed to measure the permeability of single gap junction channels for second messengers such as cAMP and ions [Hernandez et al., 2007; Ponsioen et al., 2007]. So far, only in very few studies FRET technology was used to analyze the interaction of connexins

with binding partners such as it has been shown for drebrin interaction with the Cx43 C-terminus [Butkevich et al., 2004].

In former studies we already revealed that CCN3 interacts with the C-terminus of Cx43 in the region between 257 and 382 [Gellhaus et al., 2004]. In this study we wanted to narrow down the binding site at the C-terminus of Cx43 to delineate the region of interaction with CCN3. We used sensitized FRET for interaction studies which allows multiple scanning and continuous observation of the cells to investigate the interaction properties of different C-terminal deletion constructs of Cx43 with CCN3. The results were in part unexpected. Binding of CCN3 to Cx43 was demonstrated with all constructs of the truncated Cx43-C-terminus in FRET studies but with different binding capacities. These results were fully confirmed by co-immunoprecipitation. In respect to the Cx43 C-terminus mutant (1-257) binding data differed from our previous study where we used Flag- and His-tagged constructs instead of ECFP and EYFP [Gellhaus et al., 2004] and this discrepancy may well be due to the different tags used. In a recent study Sin et al. [2009] suggest that the C-terminal residues 260–340 of Cx43 contains the CCN3 binding site(s) by using a co-immunoprecipitation competition assay with a series of Cx43 C-terminal deletion constructs in Hs578T breast cancer cells. These different findings needs further clarification and may depend on differences in the co-immunoprecipitation methods and/or cell types used.

Though binding of CCN3 with the different truncated C-termini of Cx43 was evident, the Cx43 constructs exerted different effects on proliferation and increase of CCN3 protein. As already shown for Jeg3 cells [Gellhaus et al., 2004] as well as for glioma cells [Gupta et al., 2001; Fu et al., 2004], we found a significantly reduced proliferation of human embryonic kidney epithelial 293T cells transfected with the full-length Cx43 protein. Interestingly, only the full-length Cx43 and the longest C-terminal mutant of Cx43, 1-374, but not the Cx43 constructs Cx43-257, -264, and -273, were able to reduce proliferation and correlated with increased endogenous CCN3 levels in the 293T cells. Moreover, CCN3 overexpressing Jeg3 cells but lacking the Cx43 protein showed also a significant reduction in growth [Gellhaus et al., 2004]. The findings here extend and support our previous results that Cx43 mediates its growth regulatory properties by elevating the CCN3 protein level. Thus, binding of CCN3 and Cx43 is indirectly necessary for growth reduction but only if this binding capacity leads to an increase in endogenous CCN3. CCN3 seems to be the key factor in regulating proliferation properties by a still unknown signaling cascade. Because we have shown that the shortest truncated Cx43 C-terminus (1-257) construct is still able to form functional channels [Maass et al., 2004] a failure in direct cell–cell communication by exchanging small molecules is unlikely to be responsible for changes in proliferation.

Because CCN3 needs to bind to nearly the complete C-terminus of Cx43 to fulfil its growth repressive functions, we surmise that not the binding of CCN3 at the C-terminus of Cx43 alone is sufficient to initiate growth suppression but other proteins may be then recruited which bind to the Cx43 C-terminus and are equally important.

Obviously in our study the exclusive deletion of the PDZ2 domain located at the end of the Cx43 C-terminus (Cx43-374) enhanced the binding capacity of CCN3 to Cx43 and was accompanied with induction of high levels of endogenous CCN3 and significant growth reduction. This may indicate that the PDZ2 domain has a steric inhibitory influence on CCN3 binding or that some inhibitory factor is introduced by the fluorescent protein tag at the end of the PDZ domain which influence binding with CCN3 [van Ham and Hendriks, 2003]. In addition, we cannot exclude further signaling molecules which are involved in this growth regulatory pathway of CCN3/Cx43 interaction and fail to interact with the Cx43 1-374 construct lacking eight amino acids.

This hypothesis is supported by studies of Sorgen et al. [2004] who showed that c-Src binding can disrupt the Cx43-ZO-1 interaction, leading to downregulation of gap junction intercellular communication pointing to a multimolecular complex for action. The authors showed [Sorgen et al., 2002, 2004] that the C-terminus of Cx43 primarily exists as an elongated random coil with two regions of α-helical structure. Further analysis of the interaction between Cx43-CT and c-Src SH3 domain and ZO-1 demonstrated that the SH3 domain could partially displace the Cx43-CT PDZ complex for ZO-1 interaction which means that the structural modifications brought about by this interaction are flexible [Sorgen et al., 2004]. The authors stated that a disordered C-terminus of Cx43 could control intercellular signaling between different binding partners that may be important for regulation of Cx43. In this study we cannot exclude that the known flexibility of the Cx43 C-terminus may has an effect on FRET efficiency.

In summary, binding of the C-terminus of Cx43 and CCN3 revealed that only an interaction of CCN3 with nearly the complete C-terminus of Cx43 led to an increase in CCN3 expression combined with a reduced cell proliferation. The analysis of Cx43/CCN3 interaction by FRET in 293T cells provides new insights into the interaction of these two important signaling molecules involved in cell proliferation and allows modeling the 3D structure of this complex.

ACKNOWLEDGMENTS

We would like to thank Ewa Kusch, Georgia Rauter, Gabriele Sehn, Ursula Schmücker, and Melanie Gemein for excellent technical assistance. We greatly appreciate Xuesen Dong (Mount Sinai Hospital, Toronto, Canada) for providing us with the pFlag-Cx43 and pHis-NOV/CCN3 plasmids and Jonathan W. Mueller (University Duisburg-Essen, Essen, Germany) for the pECFP-PIN1-EYFP plasmid. This work was supported by grants from the German Research Foundation [DFG: Wi 774/21-3] to Elke Winterhager and by the European Commission under the 6th Framework Programme [Contract No.: LSHM-CT-2005-018725, PULMOTENSION] to Joachim Fandrey. This publication reflects only the authors' views and the European Community is in no way liable for any use that may be made of the information contained therein.

REFERENCES

Berney C, Danuser G. 2003. FRET or no FRET: A quantitative comparison. Biophys J 84:3992–4010.

Bouvier D, Kieken F, Kellezi A, Sorgen PL. 2008. Structural changes in the carboxyl terminus of the gap junction protein connexin 40 caused by the

interaction with c-Src and zonula occludens-1. Cell Commun Adhes 15(1): 107–118.

Butkevich E, Hulsmann S, Wenzel D, Shirao T, Duden R, Majoul I. 2004. Drebrin is a novel connexin-43 binding partner that links gap junctions to the submembrane cytoskeleton. Curr Biol 14:650–658.

Chen CC, Lau LF. 2008. Functions and mechanisms of action of CCN matricellular proteins. Int J Biochem Cell Biol 41:771–783.

Chen J, Pan L, Wei Z, Zhao Y, Zhang M. 2008. Domain-swapped dimerization of ZO-1 PDZ2 generates specific and regulatory connexin43-binding sites. EMBO J 27(15): 2113–2123.

Dbouk HA, Mroue RM, El-Sabban ME, Talhouk RS. 2009. Connexins: A myriad of functions extending beyond assembly of gap junction channels. Cell Commun Signal 7:4. 10.1186/1478-811X-7-4.

Falk MM, Lauf U. 2001. High resolution, fluorescence deconvolution microscopy and tagging with the autofluorescent tracers CFP, GFP, and YFP to study the structural composition of gap junctions in living cells. Microsc Res Tech 52:251–262.

Feige JN, Sage D, Wahli W, Desvergne B, Gelman L. 2005. PixFRET, an ImageJ plug-in for FRET calculation that can accommodate variations in spectral bleed-throughs. Microsc Res Tech 68:51–58.

Fu CT, Bechberger JF, Ozok MA, Perbal N, Naus CC. 2004. CCN3 (NOV) interacts with connexin43 in C6 glioma cells: Possible mechanism of connexin-mediated growth suppression. J Biol Chem 279:36943–36950.

Gellhaus A, Dong X, Propson S, Maass K, Klein-Hitpass L, Kibschull M, Traub O, Willecke K, Perbal B, Lye SJ, Winterhager E. 2004. Connexin43 interacts with NOV: A possible mechanism for negative regulation of cell growth in choriocarcinoma cells. J Biol Chem 279:36931–36942.

Giepmans BN. 2004. Gap junctions and connexin-interacting proteins. Cardiovasc Res 62:233–245.

Giepmans BN, Moolenaar WH. 1998. The gap junction protein connexin43 interacts with the second PDZ domain of the zona occludens-1 protein. Curr Biol 8:931–934.

Giepmans BNG, Hengeveld T, Postma FR, Moolenaar WH. 2001a. Interaction of c-Src with gap junction protein connexin-43. Role in the regulation of cell-cell communication. J Biol Chem 276:8544–8549.

Giepmans BNG, Verlaan I, Hengeveld T, Janssen H, Calafat J, Falk MM, Moolenaar WH. 2001b. Gap junction protein connexin-43 interacts directly with microtubules. Curr Biol 11:1364–1368.

Gupta N, Wang H, McLeod TL, Naus CCG, Kyurkchiev S, Advani S, Yu J, Perbal B, Weichselbaum RR. 2001. Inhibition of glioma cell growth and tumorigenic potential by CCN3 (NOV). J Clin Pathol Mol Pathol 54:293–299.

Harris AL. 2007. Connexin channel permeability to cytoplasmic molecules. Prog Biophys Mol Biol 94:120–143.

Hernandez VH, Bortolozzi M, Pertegato V, Beltramello M, Giarin M, Zaccolo M, Pantano S, Mammano F. 2007. Unitary permeability of gap junction channels to second messengers measured by FRET microscopy. Nat Methods 4:353–358.

Holbourn KP, Acharya KR, Perbal B. 2008. The CCN family of proteins: Structure-function relationships. Trends Biochem Sci 33:461–473.

Hunter AW, Barker RJ, Zhu C, Gourdie RG. 2005. Zonula occludens-1 alters connexin43 gap junction size and organization by influencing channel accretion. Mol Biol Cell 16:5686–5698.

Jin C, Martyn KD, Kurata WE, Warn-Cramer BJ, Lau AF. 2004. Connexin43 PDZ2 binding domain mutants create functional gap junctions and exhibit altered phosphorylation. Cell Commun Adhes 11:67–87.

Kardami E, Dang X, Iacobas DA, Nickel BE, Jeyaraman M, Srisakuldee W, Makazan J, Tanguy S, Spray DC. 2007. The role of connexins in controlling cell growth and gene expression. Prog Biophys Mol Biol 94:245–264.

Katsube K, Sakamoto K, Tamamura Y, Yamaguchi A. 2009. Role of CCN, a vertebrate specific gene family, in development. Dev Growth Differ 51:55–67.

Katsuki Y, Sakamoto K, Minamizato T, Makino H, Umezawa A, Ikeda MA, Perbal B, Amagasa T, Yamaguchi A, Katsube K. 2008. Inhibitory effect of CT domain of CCN3/NOV on proliferation and differentiation of osteogenic mesenchymal stem cells, Kusa-A1. Biochem Biophys Res Commun 368:808–814.

Laird DW, Jordan K, Thomas T, Qin H, Fistouris P, Shao Q. 2001. Comparative analysis and application of fluorescent protein-tagged connexins. Microsc Res Tech 52:263–272.

Leask A, Abraham DJ. 2006. All in the CCN family: Essential matricellular signaling modulators emerge from the bunker. J Cell Sci 119:4803–4810.

Leithe E, Sirnes S, Omori Y, Rivedal E. 2006. Downregulation of gap junctions in cancer cells. Crit Rev Oncog 12:225–256.

Li X, Su V, Kurata WE, Jin C, Lau AF. 2008. A novel connexin43-interacting protein, CIP75, which belongs to the UbL-UBA protein family, regulates the turnover of connexin43. J Biol Chem 283:5748–5759.

Loewenstein WR. 1972. Cellular communication through membrane junctions. Special consideration of wound healing and cancer. Arch Intern Med 129:299–305.

Maass K, Ghanem A, Kim JS, Saathoff M, Urschel S, Kirfel G, Grümmer R, Kretz M, Lewalter T, Tiemann K, Winterhager E, Herzog V, Willecke K. 2004. Defective epidermal barrier in neonatal mice lacking the C-terminal region of connexin43. Mol Biol Cell 15:4597–4608.

McCallum L, Irvine AE. 2008. CCN3—A key regulator of the hematopoietic compartment. Blood Rev 23:79–85.

McLeod TL, Bechberger JF, Naus CC. 2001. Determination of a potential role of the CCN family of growth regulators in connexin43 transfected C6 glioma cells. Cell Commun Adhes 8:441–445.

Mese G, Richard G, White TW. 2007. Gap junctions: Basic structure and function. J Invest Dermatol 127:2516–2524.

Mesnil M, Crespin S, Avanzo JL, Zaidan-Dagli ML. 2005. Defective gap junctional intercellular communication in the carcinogenic process. Biochim Biophys Acta 1719:125–145.

Moorby C, Patel M. 2001. Dual functions for connexins: Cx43 regulates growth independently of gap junction formation. Exp Cell Res 271:238–248.

Moreno AP, Lau AF. 2007. Gap junction channel gating modulated through protein phosphorylation. Prog Biophys Mol Biol 94:107–119.

Patterson GH, Piston DW, Barisas BG. 2000. Forster distances between green fluorescent protein pairs. Anal Biochem 284:438–440.

Perbal B. 2004. CCN proteins: Multifunctional signaling regulators. Lancet 363:62–64.

Ponsioen B, van Zeijl L, Moolenaar WH, Jalink K. 2007. Direct measurement of cyclic AMP diffusion and signaling through connexin43 gap junctional channels. Exp Cell Res 313:415–423.

Sato H, Hagiwara H, Senba H, Fukumoto K, Nagashima Y, Yamasaki H, Ueno K, Yano T. 2008. The inhibitory effect of connexin 32 gene on metastasis in renal cell carcinoma. Mol Carcinog 47:403–409.

Sin WC, Tse M, Planque N, Perbal B, Lampe PD, Naus CC. 2009. Matricellular protein CCN3 (NOV) regulates actin cytoskeleton reorganization. J Biol Chem 284: 29935–29944.

Soehl G, Willecke A. 2003. An update on connexin genes and their nomenclature in mouse and man. Cell Commun Adhes 10:173–180.

Soehl G, Willecke A. 2004. Gap junctions and the connexin protein family. Cardiovasc Res 62:228–232.

Solan JL, Lampe PD. 2009. Connexin43 phosphorylation: Structural changes and biological effects. Biochem J 419:261–272.

Sorgen PL, Duffy HS, Cahill SM, Coombs W, Spray DC, Delmar M, Girvin ME. 2002. Sequence-specific resonance assignment of the carboxyl terminal domain of Connexin43. J Biomol NMR 23:245–246.

Sorgen PL, Duffy HS, Sahoo P, Coombs W, Delmar M, Spray DC. 2004. Structural changes in the carboxyl terminus of the gap junction protein connexin43 indicates signaling between binding domains for c-Src and zonula occludens-1. J Biol Chem 279:54695–54701.

Toyofuku T, Yabuki M, Otso K, Kuzuya T, Hori M, Tada M. 1998. Direct association of the gap junction protein connexin-43 with ZO-1 in cardiac myocytes. J Biol Chem 273:12725–12731.

Toyofuku T, Akamatsu Y, Zhang H, Kuzuya T, Tada M, Hori M. 2001. c-Src regulates the interaction between connexin-43 and ZO-1 in cardiac myocytes. J Biol Chem 276:1780–1788.

van Ham M, Hendriks W. 2003. PDZ domains-glue and guide. Mol Biol Rep 30(2): 69–82.

Willecke K, Eiberger J, von Maltzahn J. 2005. Connexins and pannexin genes in the mouse and human genome. In: Elke Winterhager, Gap junctions in development and disease. Heidelberg, Germany: Springer. pp 1–12.

Wotzlaw C, Otto T, Berchner-Pfannschmidt U, Metzen E, Acker H, Fandrey J. 2007. Optical analysis of the HIF-1 complex in living cells by FRET and FRAP. FASEB J 21:700–707.

Zacharias DA. 2002. Sticky caveats in an otherwise glowing report: Oligomerizing fluorescent proteins and their use in cell biology. Sci STKE 131: PE23.